Journal of Cosmology, 2010, Vol 8, 1846-1862
JournalofCosmology.com, June, 2010.

What is the Major Culprit for Global Warming: CFCs or CO_2?

Qing-Bin Lu, Ph.D.,
Department of Physics and Astronomy and Departments of Biology and Chemistry, University of Waterloo, Waterloo, Ontario, CANADA

ABSTRACT

A recent observation strikingly showed that global warming from 1950 to 2000 was most likely caused by the significant increase of chlorofluorocarbons (CFCs) in the Earth atmosphere (Lu, 2010). Here, three key questions are addressed: (1) How could CO_2 play a negligible role in recent global warming in view of its extremely high concentrations of $\geq$300 ppm? (2) Is there other evidence from satellite or ground measurements for the saturation in warming effect of CO_2 and other non-CFC gases? And (3) could the greenhouse effect of CFCs alone account for the rise of 0.5~0.6 K in global temperature since 1950? First, the essential feature of the Earth blackbody radiation is elucidated. Then re-analyses of observed data about global temperature change with variations of halocarbons and CO_2, the atmospheric transmittance of the infrared radiation and the 1970-1997 change in outgoing longwave radiation spectra of the Earth are presented. It follows by new theoretical calculations of the greenhouse effect of halocarbons. The results strength the conclusion that humans were responsible for global warming in late 20th century, but CFCs, rather than CO_2, were the major culprit; a long-term global cooling starting around 2002 is expected to continue for next five to seven decades.

Key words: Global warming; Global cooling; Chlorofluorocarbons (CFCs); CO_2; Ozone hole

1. Introduction

Climate models (IPCC, 2001, 2007) have concluded that CO_2 plays a major role in global warming observed in the late 20th century, based on the large radiative force of CO_2 calculated from its dominantly high concentrations of $\geq$300 ppm. However, there seem an increasing number of studies which show that the main mechanism of global warming remains elusive (e.g., Friis-Christensen and Lassen, 1991; Balling, 1992; Svensmark and Friis-Christensen, 1997; Lindzen, 1997; Idso, 1998; Veizer et al., 2000; Soon et al., 2001; Carslaw et al., 2002; Douglass et al., 2004, etc.). A recent study (Lu, 2010) strikingly showed that the 11-year cyclic variations of ozone loss and temperature data in the lower stratosphere over Antarctica from the 1950s to 2008 can be well reproduced by a simple relationship governed by halocarbons (mainly CFCs) and cosmic rays only. That observation did not agree with the predictions of stratospheric cooling and enhanced ozone loss due to *increasing* non-CFC greenhouse gases in climate models (Austin et al., 1992; Shindell et al., 1998; WMO, 1999). An excellent linear dependence was also found between global surface temperature and the total loading of atmospheric CFCs with small modulations by 11-year cycles of cosmic ray intensity. One

striking consequence is that as the total level of atmospheric CFCs was estimated to decline since around 2000 with a 6(±3)-year delay Γ from the measured peak at the surface (WMO, 2007), global temperature has correspondingly decreased since ~2002 (Lu, 2010). In contrast, the concentration of atmospheric CO_2 has kept rising since the industrial revolution. *These observations have pointed to the striking possibility that global warming observed in the period of 1950 to 2000 was caused by the significant appearance of CFCs in the atmosphere* (Lu, 2010).

Although it is long known that $CFCl_3$ (CFC11) and CF_2Cl_2 (CFC12) are effective greenhouse gases (Ramanathan, 1975, 1985; Wang and Molnar, 1985; WMO, 1999, 2007), it has been generally thought that CFCs would play only a minor part in global warming because their concentrations (≤540 ppt) are three to six orders of magnitude lower than those of non-CFC greenhouse gases (CO_2, CH_4 and N_2O) (Ramanathan,1998; IPCC, 2001, 2007). Thus, there apparently exist three puzzling questions. First, how could CO_2 and other non-CFC greenhouse gases play a negligible role in the 1950-2000 global warming in spite of their extremely high concentrations? Second, is there other evidence from satellite or ground measurements for the almost zero warming effect of increasing CO_2? Third, can the greenhouse effect of CFCs be large enough to account for the rise of 0.5~0.6 K in global temperature since 1950? This paper will address all the three questions.

2. The Wien peak of earth's blackbody radiation

The radiation of the Earth surface after absorbing solar radiation can approximately be treated as a blackbody radiation. The radiation power in the wavelength interval dλ or the frequency interval dν is given by the Planck formula:

$$B_\lambda(T)d\lambda = \frac{8\pi hcV}{\lambda^5(e^{hc/\lambda kT}-1)}d\lambda, \quad \text{or} \quad B_\nu(T)d\nu = \frac{8\pi hV\nu^3}{c^3(e^{h\nu/kT}-1)}d\nu, \tag{1}$$

where $B_\lambda(T)$ and $B_\nu(T)$ are the power density defined as the intensity I (radiation energy per unit time per unit area) per unit wavelength λ and as the intensity I per unit frequency ν (=c/λ), respectively. Traditionally the Wien's displacement law gives the wavelength λ_{max} at which $B_\lambda(T)$ is at the maximum by λ_{max}=2898 μm.K/T. Given that the Earth surface temperature is about 300 K, $B_\lambda(T)$ will have a peak at λ_{max}=9.66 μm in the infra-red (IR) wavelength range. Since IR absorption spectra of molecules are usually measured by an IR spectrometer that uses a Fourier transform method, the radiance spectrum of the Earth is often presented as a function of wavenumber (1/λ) in cm^{-1}. When $B_\nu(T)$ is applied, one obtains that $B_\nu(T)$ peaks at the wavenumber around 588 cm^{-1}, corresponding to the wavelength of 17.0 μm. As shown in Fig. 1a, the wavelength corresponding to the $B_\nu(T)$ peak is 1.76 longer than the wavelength λ_{max} at which $B_\lambda(T)$ peaks for any blackbody temperature. Since CO_2 happens to have a strong absorption band at 600-770 cm^{-1} (13-17 μm), it was thought that the blackbody radiation intensity of the Earth centers at the absorption band of CO_2 (Ramanathan, 1998). This is, however, a misconception, and is similar to say that the Sun has a radiation peak at 880 nm (in the near IR region) derived from $B_\nu(T)$ rather than at the well-known visible wavelength of ~500 nm obtained from $B_\lambda(T)$ using the Wien displacement law. In fact, it is misleading to compare either of the Planck function peaks in Fig. 1a with the atmospheric absorption (transmittance) spectrum, since they are drastically different in physical nature. Similar to previous studies of

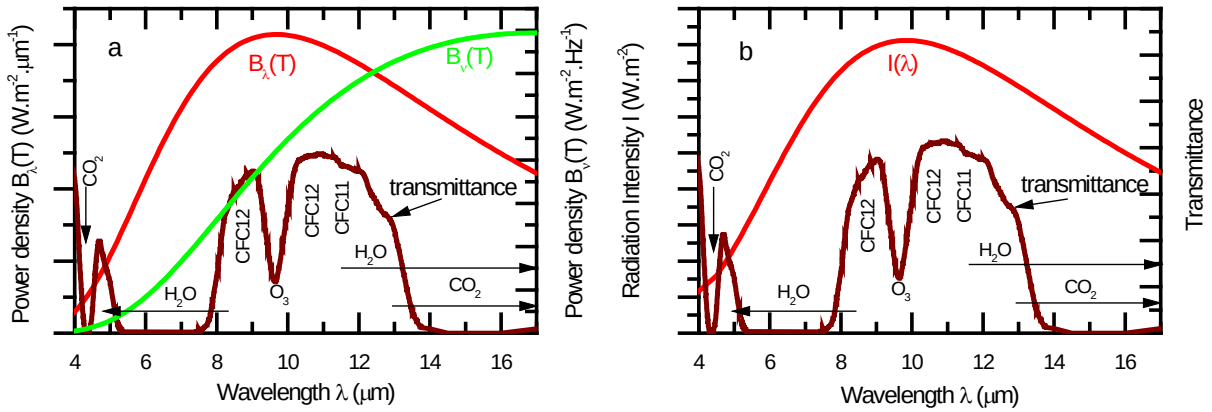

Figure 1. Earth's blackbody radiation spectrum and atmospheric transmittance spectrum. *a*: Radiation power density of Earth blackbody, expressed as the intensity I (radiation energy per unit time per unit area) per unit wavelength λ — $B_\lambda(T)$ and as the intensity I per unit frequency ν — $B_\nu(T)$, as a function of wavelength λ. *b*: Intensity spectrum I(λ) obtained by integration of $B_\lambda(T)$ over a wavelength interval Δλ=3 μm or by integration of $B_\nu(T)$ over the corresponding frequency interval $\Delta\nu=(c/\lambda^2)\Delta\lambda$. Also shown is a theoretical atmospheric transmittance spectrum obtained with Modtran4 calculations (Ratkowski et al., 1998).

the solar Wien peak (Soffer and Lynch, 1999; Overduin, 2003), this paradox can be solved with the integral of either $B_\lambda(T)$ over λ or $B_\nu(T)$ over ν, which must give the same intensity I. This comes directly from their definitions: $B_\lambda(T)d\lambda=B_\nu(T)d\nu$. The intensity spectrum I(λ) can be obtaining by integrating the $B_\lambda(T)$ over a certain wavelength interval Δλ (Overduin, 2003):

$$I(\lambda)=\int_{\lambda-\Delta\lambda/2}^{\lambda+\Delta\lambda/2}B_\lambda(T)d\lambda. \qquad (2)$$

The results are plotted in Fig. 1b as a function of λ over the wavelength range of 4-17 μm for a wavelength interval of Δλ=3 μm. The integration of $B_\nu(T)$ over the corresponding frequency interval $\Delta\nu=(-c/\lambda^2)\,\Delta\lambda$ produces exactly the same intensity curve peaking at around 10 μm.

In fact, the spectral region of 8-12 μm is generally called as the atmospheric "window". There are two reasons for this identification. First, the unpolluted atmosphere in this spectral region is quite transparent, except for the absorption by ozone in the 9.6 μm band, as seen from the modeled transmittance spectrum shown in Fig. 1. This is the argument often taken by atmospheric climatologists (Ramanathan et al., 1975, 1998). Second, as shown in Fig. 1b, the majority of the Earth radiation energy is emitted into space through the 8-12 μm spectral region in which the maximum radiation intensity locates. Overall, both facts lead to the conclusion that nearly 80% of the total radiation energy from the surface and clouds is emitted into space in the 8-12 μm region. As a consequence, any polluting molecule with a strong absorption in the 8 to 12 μm region is highly effective in generating greenhouse effect. Unfortunately, many halogenated molecules such as CFC11 ($CFCl_3$) and CFC12 (CF_2Cl_2) are not only ozone-depleting molecules but also highly effective greenhouse effects, since they have strong absorption bands in the 8 to 12 μm region (Ramanathan et al., 1975, 1985; Wang and Molnar, 1985). As shown in Fig. 1, CO_2 contributes to the strong absorption bands at 4-5 μm and 13-17 μm, while H_2O is the effective absorber in the entire infrared spectral range and has two major bands at 5-8.3 μm and 11-17 μm. Here, the key questions are how serious the greenhouse effect of CFCs is, compared with that of non-CFC gases (particularly CO_2), and if there is

saturation in the warming effect of non-CFC gases in view of their extremely high concentrations in hundreds of ppb to ppm.

3. Evidence of the saturation effect of non-CFC greenhouse gases

A. Global surface temperatures. It was recently observed that global surface temperature kept nearly constant form 1850 to ~1950, while the recorded CO_2 level had increased linearly since 1850 (Lu, 2010). This is now more clearly shown in Fig. 2, where the data in 1930-1950 are not included to avoid any potential effects of the World War II. Global temperature is plotted versus CO_2 concentration in Fig. 2b, which gives rise to a nearly zero correlation coefficient R (=0.02). *That is, the global temperature was independent of the rising CO_2 level (285 to 307 ppm) in the period of eight decades.* It was also found that the southern hemisphere and global surface temperatures have decreased since ~2002 (Lu, 2010). One might argue that these temperature drops are just short-term and due to the 11-year cycle of cosmic rays or the solar activity. To clarify this issue, time-series data of atmospheric CO_2 concentration, the total concentration of major atmospheric halocarbons (CFCs, CCl_4 and HCFCs) and global surface temperature over nearly six decades from 1950 to 2009 are plotted in Figs. 3a and b, respectively. It can be seen from Fig. 3b that global surface temperature was nearly constant from 1950 to ~1975, then had a linear rise from 1975 to ~2002 and finally turned to decrease after 2002. Moreover, Figs. 3c and d plot global temperature as a function of total concentration of halocarbons and CO_2 concentration, respectively. In Figs. 3a and c, a delay Γ=9 year of halocarbon concentrations in the tropopause and stratosphere from surface measurements must be applied (Lu, 2010; WMO, 2007); otherwise global surface temperature would show a *sharp rise* with higher total halocarbon concentrations above 1100 ppt (≥1.1 ppb). Strikingly, Fig. 3c shows that global surface temperature has an excellent positive linear correlation with the total loading of halocarbons in the atmosphere from the 1950 to the present; *a linear fit gives a statistical correlation coefficient R as high as 0.96*. Fig. 3d exhibits a similar behavior to Fig. 3b for global temperature change with increasing CO_2 concentrations: the temperature did not

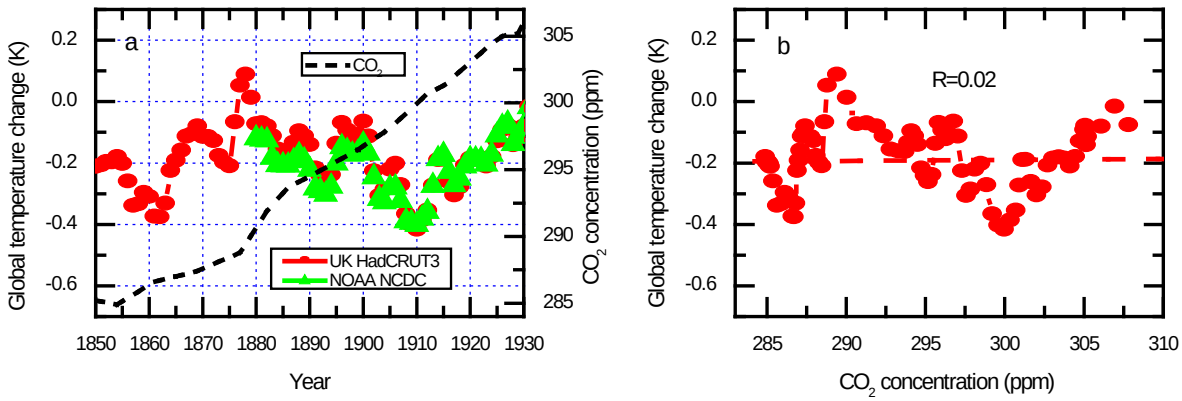

Figure 2. Global surface temperature and CO_2 level from 1850 to 1930. *a*: Time-series variations of atmospheric CO_2 concentration and global surface temperature. *b*: Global surface temperatures versus atmospheric CO_2 concentration; a nearly zero correlation coefficient R(=0.02) was obtained from the curve fit. CO_2 data were from the Law Dome ice core analysis**.** Global surface temperature data were from both the UK Met Office Hadley Centre and the NCDC of the US NOAA; only a minimum 3-point smoothing was applied to observed data.

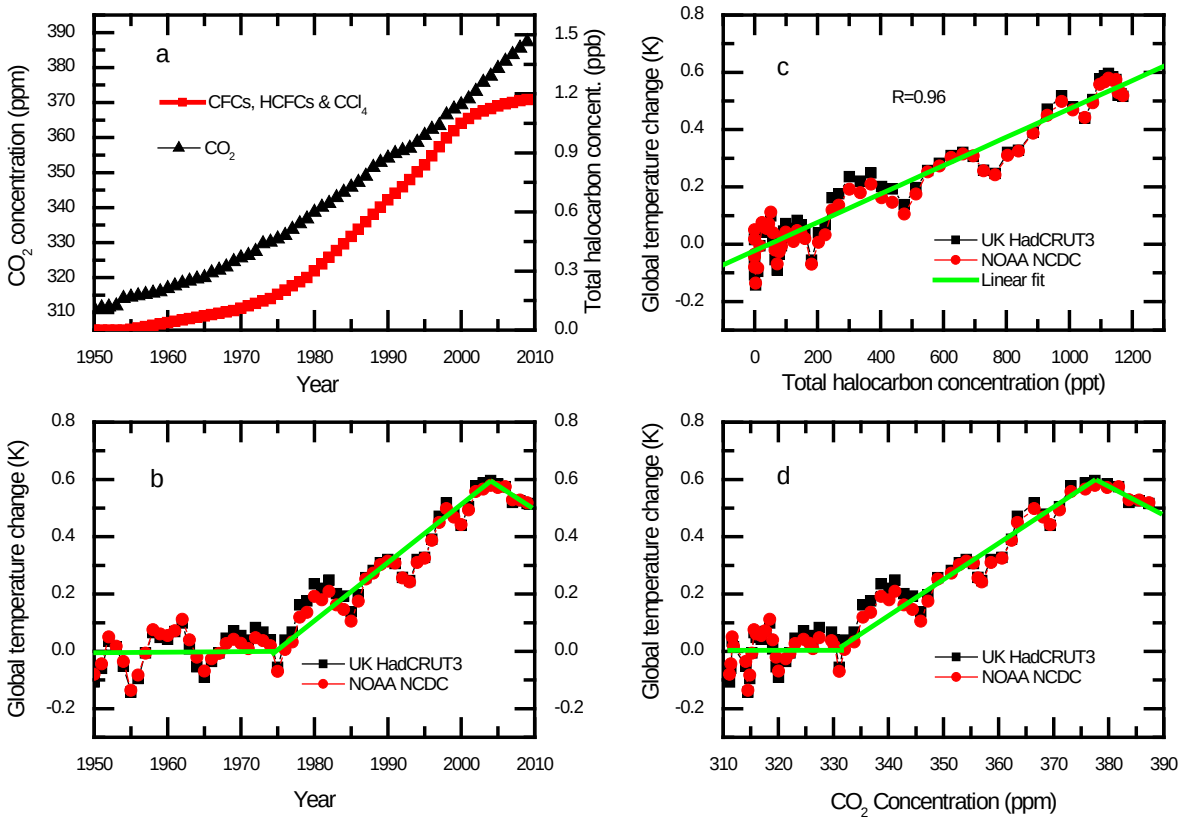

Figure 3. Global surface temperature, CO_2 and halocarbon levels from 1950 to 2009. *a-b*: Time-series variations of atmospheric CO_2 concentration, the total concentration of atmospheric halocarbons (CFCs, HCFCs and CCl_4) and global surface temperature. *c-d*: Global temperatures versus concentrations of atmospheric halocarbons and CO_2, respectively. CO_2 data were obtained from direct atmospheric measurements at Mauna Loa Observatory, Hawaii**;** halocarbon concentrations were obtained from the WMO Report (2007). In *a* and *c*, the total concentrations of atmospheric halocarbons are adjusted by a time delay Γ= 9 year from surface measurements (Lu, 2010; WMO, 2007). Temperature data were from the same sources as in Figure 2; only a minimum 3-point smoothing was applied to observed data.

rise appreciably for 310-330 ppm CO_2, then appeared to have a linear increase up to the CO_2 concentration of 377 ppm, and finally started to decrease with higher CO_2 levels $\geq$377 ppm after ~2002. At first glimpse, one might be attempted to conclude that CO_2 was the driving force for the temperature increase from 1975 to ~2002. However, this assignment contradicts with the observations for 1850–1930 and 1950–1975 (Fig. 2 and Fig. 3), showing no temperature rise once no significant atmospheric CFCs, and for 2002 to the present, showing a *decrease* in global temperature with rising atmospheric CO_2 levels. As more clearly shown in Fig. 3, small oscillations in global temperature with a regular periodicity of 11 years cannot account for the significant temperature drop since ~2002. In fact, these small *periodic* oscillations seem not be due to a direct effect of either cosmic rays or the solar activity because it did not appear in measured temperatures from 1850 to 1930 (Fig. 2a), during which atmospheric halocarbon concentrations were essentially zero (Fig. 3a). Instead, observed small oscillations in global temperature are more likely due to ozone loss caused by co-effects of CFCs and cosmic rays (Lu, 2010). The data in Figs. 2 and 3 strongly indicate that global temperature is highly sensitive to the variation of atmospheric CFCs (and HCFCs) rather than to increasing CO_2 and other non-CFC greenhouse gases. In the high concentration range of ppm, CO_2 should exhibit higher climate sensitivities at lower concentrations. There is no reason to argue that global

temperature would have an almost zero sensitivity to CO_2 in the concentration range of 285-330 ppm and then have a linear dependence on CO_2 in the range of 330-377 ppm. In striking contrast, global temperature has exhibited an excellent linear positive correlation with the total concentration of halocarbons since their initial emission into the atmosphere in the 1950s. All these observations indicate that the warming effect of increasing non-CFC gases is most likely to have saturated.

B. Atmospheric transmittance spectra. Figure 4 shows two atmospheric transmittance spectra obtained from measurements on the ADEOS satellite in 1997 (Kobayashi et al., 1999; Clerbaux et al., 2003) and on Mount Miron at 30° ground-to-space slant path using the rising Sun as a radiation source in 1990, as well as a theoretical transmittance spectrum from

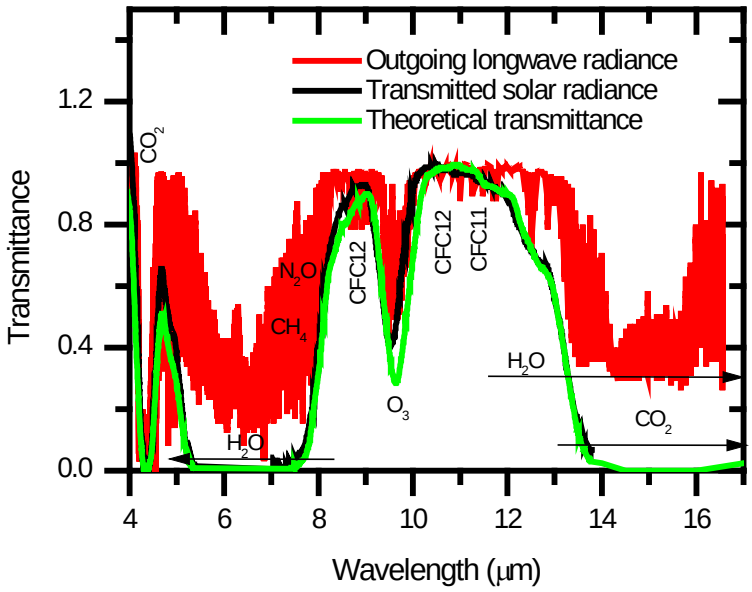

Figure 4. Calculated and measured atmospheric transmittance spectra. Measured spectra were from measurements of outgoing longwave radiation (OLR) by the IMG onboard on the ADEOS satellite (Clerbaux et al., 2003) and of the transmitted spectral radiance of the Sun as a blackbody source on Mount Miron at 30° ground-to-space slant path (Ratkowski et al., 1998). For the latter, the modeled atmospheric transmittance was from Modtran 4 calculations. Modeled and measured solar transmittance spectra were normalized to the maximum transmittance of the measured OLR transmittance spectrum in the 8-12 μm 'atmospheric window'.

Modtran4 simulations for the latter measurements by Ratkowski et al. (1998). The Interferometric Monitor of Greenhouse Gases (IMG) instrument onboard the ADEOS satellite measured the outgoing longwave radiation (OLR) of the Earth blackbody at the top of the atmosphere, while the ground measurement gave the transmitted spectral radiance of the Sun as a blackbody source. As the modeled and measured solar transmittance spectra are normalized to the maximum transmittance measured from the OLR (IMG) in the atmospheric window, the transmittances from the two measurements at the O_3 band overlap fairly well. The O_3 absorption in the 1997 IMG spectrum is slightly weaker than that in the 1990 solar spectrum. This is reasonable, as the total ozone in global stratosphere in 1997 was a few percent lower than that in 1990 (Lu, 2009). This indicates that ground and satellite measurements are comparable. It can also be seen that the measured solar transmittance spectrum is in excellent agreement with the simulated spectrum, particularly in the spectral region of ≥11.5 μm, which is

at the heart of the current debate. It is clear that the absorption by CO_2 is so strong that the transmittance is zero in the 4-5 μm spectral region, measured on either the satellite or the ground. Remarkably, both simulated and measured transmittances in the 13-17 μm spectral region using the Sun as a source are also zero, while it was measured to be non-zero at the top of the atmosphere by the IMG. Understanding this difference is of particular significance. The climate models (Ramanathan, 1998; IPCC, 2001, 2007) assume that the radiative force of CO_2 would increase logarithmically with rising CO_2 concentration, that is, the IR radiation at the CO_2 absorption bands from the Earth surface would still be transmissive through the atmosphere. It is a particularly good approximation in the IR spectral region that scattering is negligible; the radiative transfer in the atmosphere is then given by the Schwarzchild's equation (Kidder and Vonder Haar, 1995). The latter gives that the measured OLR flux F_{out} at the top of the atmosphere includes two contributions: the transmitted IR radiation $\rho_t F_S$ from the Earth surface and the fluorescence emission F_f of IR-adsorbed CO_2 in the atmosphere:

$$F_{out}=\rho_t F_S+F_f. \quad (3)$$

Here F_S and ρ_t are the upward radiation flux of the ground and its transmittance in the atmosphere, respectively. And the Kirchhoff's law gives

$$F_f=(1-\rho_t)\sigma T_a^4, \quad (4)$$

where T_a is the equivalent blackbody temperature of the atmosphere. Nevertheless, calculations using Lambert-Beer's law with measured absorption coefficients / band intensities [~10 cm^{-1} atm^{-1} (Ramanathan et al., 1985; Schneider, 1989)] and concentrations (300-380 ppm) of CO_2, as included in Modtran 4, simply give zero transmittance $\rho_t \approx 0$ even at the very low troposphere at the IR regions of 4-5 μm and 13-17μm. This is in excellent agreement with the measured solar transmittance spectrum on the ground, as shown in Fig. 4. This consistency demonstrates that the observed non-zero transmittance in the CO_2 13-17 μm band at the top of the atmosphere is solely due to the fluorescence radiation of IR-adsorbed CO_2 molecules, i.e., $\rho_t = 0$ ($F_{out}=F_f$). Indeed, this was also revealed in simulated transmittance spectra with Modtran4 calculations by Berk *et al*. (1989), demonstrating that the effect of doubling CO_2 is extremely small compared to the absorption due to water (Clark, 1999). If we only consider the effect of increasing CO_2 concentration with $\rho_t=0$, the simple model of the greenhouse effect will then give the OLR flux at the top of the atmosphere by

$$F_{out}=F_f=\sigma T_a^4=F_0, \quad (5)$$

and the upward radiation flux of the ground by

$$F_S=\sigma T_S^4=F_0(1+\rho_0), \quad (6)$$

where F_0 is the unreflected incoming solar flux and ρ_0 the transmittance of incident (short-wave) solar radiation in the atmosphere (Andrews, 2000). With rising CO_2 concentrations, both surface temperature T_S and the OLR flux F_{out} (radiance) will not increase because ρ_0 is nearly constant or becomes slightly smaller. Thus, there is saturation in the warming effect of CO_2. As shown in Fig. 4, this is probably true not only for CO_2 but also for CH_4 and N_2O since these non-CFC gases have high atmospheric concentrations in 320-385 ppm, 1.5-1.8 ppm and 300-325 ppb, respectively, being 10^6, 10^4 and 10^3 times those of CFCs and HCFCs in 100-500 ppt (WMO, 2007). Note that IR absorption band strengths of CH_4 at 7.6 μm and N_2O at 7.8 μm are one to two orders of magnitudes higher than that of CO_2 at 15 μm (Ramanathan et al., 1985),

leading to the saturation in atmospheric absorption of the Earth IR radiation in these spectral regions (ρ_t=0).

C. Outgoing longwave radiation (OLR) spectra. Researchers have also realized that changes in the Earth's greenhouse effect can be detected from variations in the radiance spectrum of outgoing longwave radiation, which can be a measure of how the Earth radiation emits to space and carries the signature of greenhouse gases that cause the warming effect (Goody et al., 1998; Harries et al., 2001; Anderson et al., 2004; Griggs and Harries, 2007). Harries et al. (2001) investigated the difference spectrum between the spectra of the OLR of the Earth as measured by the NASA Infrared Interferometric Spectrometer (IRIS) onboard the Nimbus 4 spacecraft in 1970 (Hanel et al., 1971) and the IMG instrument onboard the ADEOS satellite in

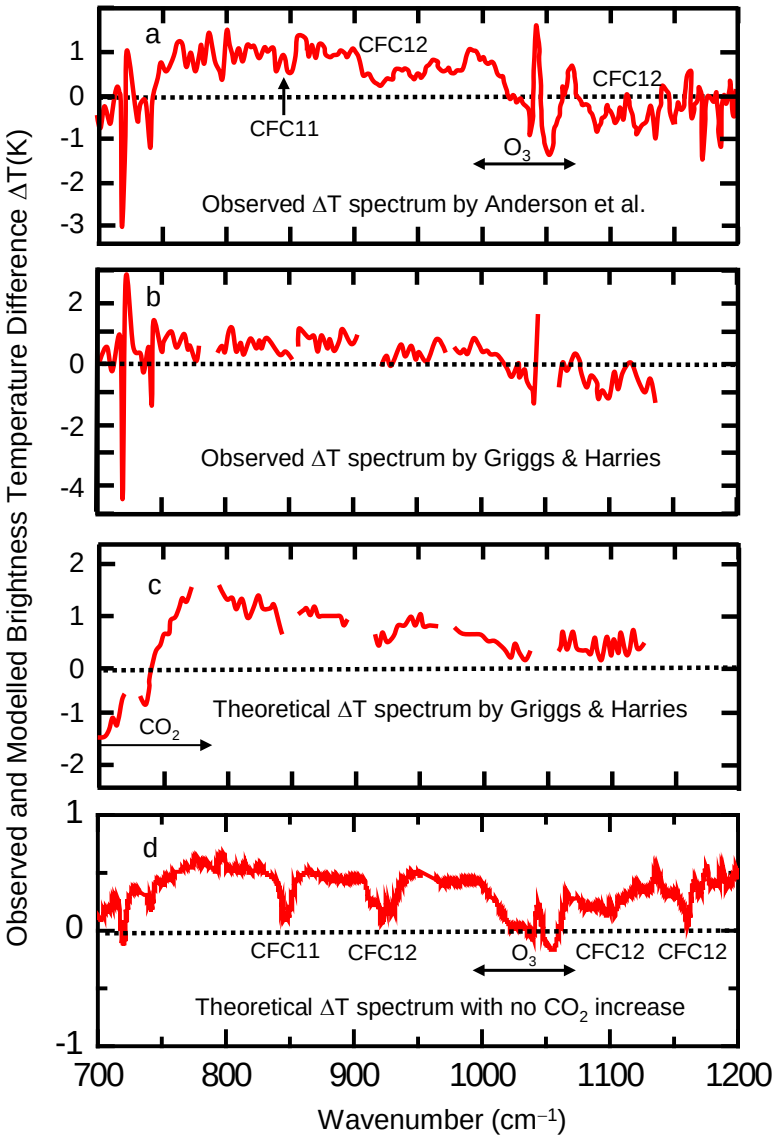

Figure 5. Observed and theoretical difference spectrum of outgoing longwave radiation for IMG-IRIS. *a* and *b*: Observations by Anderson et al. (2004) and by Griggs and Harries (2007); *c*: Simulated difference spectrum from Griggs and Harries (2007); *d*: Simulated difference spectrum with the CO_2 concentration kept unchanged at the 1970 value (the present study).

1997 (Kobayashi et al., 1999). They showed differences in the spectra associated with long-term changes in atmospheric CO_2, CH_4 and O_3 as well as CFC-11 and CFC-12, consistent with their theoretical calculations of the radiative forcing of increasing greenhouse gases expected by the climate models, over the 27-year period of most significant global warming. Subsequently, however, Anderson et al. (2004) showed that to sample the radiation field reliably requires averages over ~10^4 independent radiance spectra. They achieved a more reliable analysis of the radiance spectra in the entire tropical belt between 30° N and 30° S measured by IRIS and IMG by increasing the data sample number to 2~3x10^4 spectra and applying an innovative method averaging the spectra via 'dof weighted cells'. These improvements significantly reduced the random and system errors. Interestingly, Anderson et al. (2004) then observed the striking contrast between observed and predicted radiance spectra. As shown in Fig. 5a, most strikingly, the expected strong CO_2 absorption band in the 700 to 800 cm^{-1} region is absent in the observed difference spectrum. More recently, Griggs and Harries (2007) re-analyzed the radiance spectra of IRIS and IMG and re-calculated the radiance spectra. Their new results are very close to those obtained by Anderson et al., as shown in Figs. 5b and c. These data strikingly show that the expected strong CO_2 absorption band in the 700 to 800 cm^{-1} region does not appear in the observations of the difference radiance spectrum between 1970 and 1997 (Anderson et al., 2004; Griggs and Harries, 2007).

This radiative forcing arising from the CO_2 absorption has lied at the heart of the debate on the anthropogenic global warming observed in the late half of the 20th century. Thus, it is necessary to make a new theoretical calculation of the difference (IMG-IRIS) spectrum in the spectral rang covering the CO_2 absorption band (700 to 800 cm^{-1}) and the atmospheric window (800 to 1200 cm^{-1}), assuming that the CO_2 concentration is kept at the 1970 value. Such a difference radiance spectrum can be obtained from the simulations of the radiance spectra for 1970 and 1997 with Modtran3 (Wang et al., 1996), similar to previous simulations (Anderson et al., 2004; Griggs and Harries, 2007). The thus calculated difference (IMG-IRIS) spectrum is shown in Fig. 5d, in which all the main features due to changes in CFC11, CFC12 and O_3 in the observed difference spectrum are well reproduced. Even the simulated difference spectrum underestimates the observed absorption band of CFC12 in the region of 1080-1200 cm^{-1}. But this could be due to the uncertainties in the effects of water vapor and clouds (Ratkowski et al., 1998; Anderson et al., 2004; Griggs and Harries, 2007). Strikingly, the simulated difference spectrum now shows a satisfactory agreement with the observation, particularly in the spectral region of 700 to 800 cm^{-1}. These observations and calculations of radiance spectra therefore also provide strong evidence of the saturation in the warming effect of CO_2.

D. No effect of increasing non-CFC greenhouse gases on polar ozone loss. In fact, the absence of the greenhouse effect of increasing non-CFC gases lies not only in observed results shown in Figs. 2-5 but also in the observed 11-year cyclic variation of stratospheric cooling over Antarctica in the past five decades, as found recently (Lu, 2010). The latter data showed that the 11-year cyclic change of stratospheric temperature over Antarctica depends solely on the variation of total ozone, which can be given by a simple equation with the stratospheric level of CFCs and the intensity of cosmic rays as the only two variables. This fact indicates no effects of non-CFC greenhouse gases on stratospheric climate of Antarctica over the past five decades. This is in striking contrast to the predictions of climate models simulating the effect of increasing non-CFC greenhouse gases on polar stratospheric ozone (Austin et al., 1992; Shindell et al., 1998). For instance, those models predicted that the Antarctic and Arctic temperatures would several K colder due to stratospheric cooling induced by non-CFC greenhouse gases. It was also predicted that the ozone loss over Arctic would become very severe, nearly doubling the ozone depletion area and the ozone loss by 2000-2009, relative to

the observed values in 1990-1999 (Shindell et al., 1998). Lower-stratospheric cooling induced by increasing greenhouse gases was also predicted to expand the ozone-hole area over Antarctica in 2000-2009, though the changes would be less drastic than the Arctic ozone. Remarkably, it was also noted that without climate forcing from increasing non-CFC greenhouse gases, the average Arctic ozone loss would only change due to changes in chlorine amounts (Shindell et al., 1998). Since the equivalent effective stratospheric chlorine (EESC) level in the 2000-2009 was close to those observed in the late 1990s (1998-1999) (WMO, 2007), the predicted much greater mean Arctic ozone loss would then display the distinct signature of stratospheric cooling induced by increasing non-CFC greenhouse gases (Shindell et al., 1998). Unfortunately, the predicted results did not agree with observed data of ozone over Arctic and Antarctica in the past decade. In particular, the current Arctic ozone loss is no greater than that one decade ago. This fact, in turn, indicates no climate forcing from increasing non-CFC greenhouse gases. Moreover, the stratospheric cooling effect induced by non-CFC greenhouse gases, if exists, would be clearly observed in the stratospheric ozone and temperature data over Antarctica, with significant increases of these gas concentrations over the past five decades. In striking contrast, observed data show no effect of increasing non-CFC greenhouse gases on polar stratospheric ozone loss and cooling.

All the above observations (A-D) lead to the conclusion that increasing CO_2 and other non-CFC gases have caused no significant warming effect since the 1950s. Then, a question follows: Can the greenhouse effect of CFCs alone account for the observed surface temperature rise from the 1950s to ~2000? This is addressed in the following section.

4. Reevaluation of the greenhouse effect of CFCs

Halocarbons released from the Earth's surface become mixed in the lower atmosphere and are transported into the stratosphere by normal air circulation patterns. As shown in Figs. 1 and 4, halocarbons generally have strong absorption features in the atmospheric window in the 8-12 μm region where there is little absorption by intrinsic atmospheric gases. This absorption reduces the amount of the transmitted IR radiation from the Earth surface and leads to a direct radiative forcing. It is this forcing that can potentially play an important role in global warming. The IPCC Report (2007*)* has concluded that the increases in concentrations of halocarbons produced a maximum radiative forcing of 0.34 ± 0.03 W/m² by the year of ~2005, which represents only about 21% of the total calculated radiative forcing (1.6 W/m²) from increases in well-mixed greenhouse gases (mainly CO_2). This conclusion, however, was made with the assumption of no saturation in the greenhouse effect of non-CFC gases. The observed results discussed above strongly indicate that the greenhouse effect of non-CFC gases has saturated. Thus, one should reevaluate the actual role of CFCs in global climate change.

The magnitude of the greenhouse effect depends on the sensitivity of the climate system to changes in the radiative force of greenhouse gases. There exists a large uncertainty in *climate sensitivity factor* α, which is here defined as the amount of temperature change per change in direct radiative forcing driven by greenhouse gases, i.e. $\alpha = dT/dF$, with no climate feedback included. In climate models (IPCC, 2001, 2007), equilibrium climate sensitivity was often determined by projecting ΔT_{2x} to be a particular value corresponding to a *calculated* radiative force of $\Delta F \approx 3.7$ W/m^2 arising from a doubling of atmospheric CO_2 concentration (no saturation was assumed). The ΔT_{2x} value was therefore termed *climate sensitivity*. On the basis of studies with general circulation models, the IPCC Report (2007) estimated the range of ΔT_{2x} to be 2 K to 4.5 K with a best estimate of about 3 K. Tabulated in the IPCC Report (2007), however, a number of model estimates of 'equilibrium climate sensitivity' based on

observational temperature data gave a wide range of 1.0 K to 11.8 K with climate feedbacks included. An equilibrium temperature change of 1 K to 10 K due to a radiative force of ΔF=3.7 W/m^2 would give rise to a range of climate sensitivity factor α to be 0.135-1.35 K/(Wm^{-2}), assuming that the water vapor feedback doubles the direct warming by greenhouse gases (IPCC, 2007).

Atmospheric feedbacks largely control climate sensitivity. As global average temperature increases, tropospheric water vapor concentrations increase and this represents a key positive feedback of climate change. Water vapor changes represent the largest feedback affecting equilibrium climate sensitivity and are now better understood than two decades ago, though cloud feedbacks remain the largest source of uncertainty. It has been estimated that *water vapor feedback acting alone approximately doubles the warming from what it would be for fixed water vapour* (IPCC, 2007). Furthermore, water vapour feedback can also amplify other feedbacks such as cloud feedback and ice albedo feedback in models. If cloud feedback is strongly positive, water vapor feedback can lead to an amplification factor β of 3.5 (IPCC, 2007).

The change in equilibrium surface temperature (ΔT_s) arising from the radiative forcing ΔF of the surface-atmosphere system due solely to a trace gas increase can be calculated by:

$$\Delta T_s=\alpha\beta\Delta F, \tag{7}$$

where α is the climate sensitivity factor in K/(W/m^2), β is the amplification factor of water feedbacks. Moreover, the radiation change at the tropopause caused by a given change in greenhouse gas concentration is referred to as radiative efficiency χ, which has a unit of Wm^{-2} ppb^{-1} (WMO, 2007). The χ values are calculated using radiative transfer models of the atmosphere and depends upon the strength and spectral position of a compound's absorption bands. Radiative efficiency χ can be used to calculate the change ΔF as a function of changing concentration. For a greenhouse gas at low concentrations ($\leq$1 ppb) such as CFCs and HCFCs, ΔF has a simple linear dependence:

$$\Delta F=\chi C, \tag{8}$$

where C is the concentration of the greenhouse gas (IPCC, 2001). This has been well justified by the observed results in Fig. 3c. In present calculations, the lower limit (0.135 K W^{-1}m^2), upper limit (1.35 K W^{-1}m^2) and an intermediate value (0.9 K W^{-1}m^2) in climate sensitivity factor α and the amplification factor β=2.0 by water vapor feedback (IPCC, 2007) are used to calculate the surface equilibrium temperature change ΔT_s induced by the total greenhouse effect of CFCs, HCFCs and CCl_4. With available radiative efficiencies and (measured and projected) concentrations of these major halocarbons (WMO, 2007), the global surface temperature change ΔT_s from 1960 to 2060 calculated from Eqs. (7) and (8) are shown in Fig. 6. These calculations do not include the radiative force due to the destruction of stratospheric ozone by CFCs, which has been re-evaluated to be –0.05 [±0.10] Wm^{-2} in the IPCC Report (2007). This small negative radiative force can be well balanced by the positive radiative force arising from other halocarbons such as CH_3Cl_3 and CH_3Cl, which are not included in the present calculations. Figure 6 shows that the observed temperature change lies well between the lower limit and the upper limit of the climate sensitivity factor α with the estimated amplification factor β given in the IPCC Report. Indeed, the calculated results with α=0.9 K W^{-1}m^2 and β=2.0 reproduce the observed data the best. *These calculations demonstrate that CFCs alone could indeed account for the observed temperature rise of 0.5~0.6 K from 1950 to 2000*. The calculated data also show that global temperature will reverse slowly with a deceasing rate

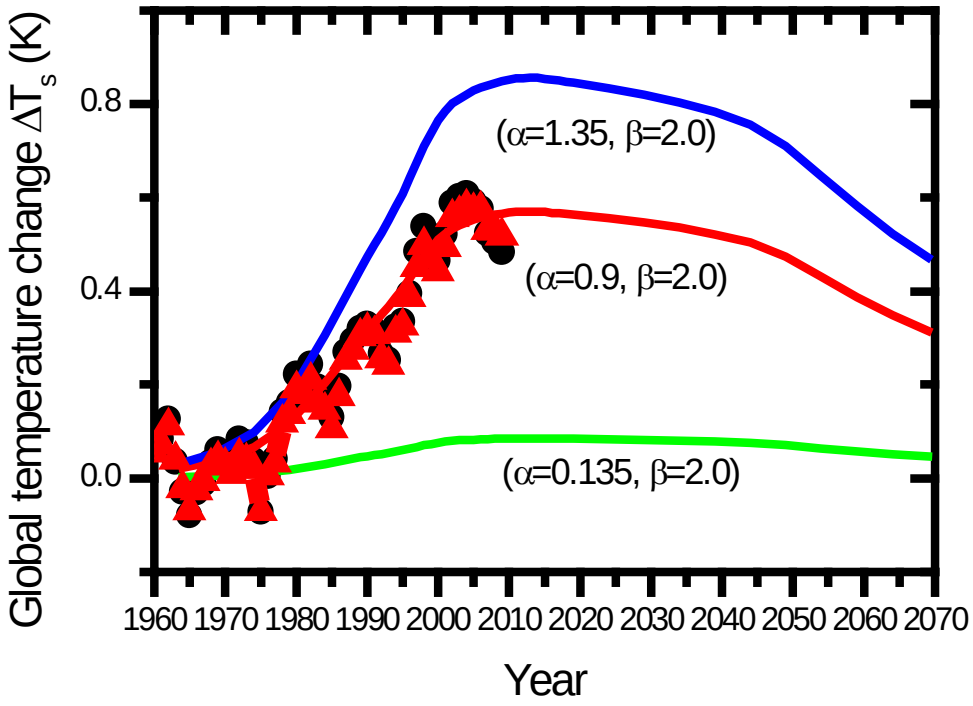

Figure 6. Calculated change in equilibrium surface temperature (ΔT_s) due solely to the greenhouse effect of CFCs, HCFCs and CCl_4, with the lower limit (0.135 K $W^{-1}m^2$), upper limit (1.35 K $W^{-1}m^2$) and an intermediate value (0.9 K $W^{-1}m^2$) in climate sensitivity factor α and the climate feedback amplification factor β=2. Same as Figure 3, atmospheric halocarbon concentrations are adjusted by a time delay Γ= 9 year from surface measurements (Lu, 2010; WMO, 2007). Observed surface temperature data (symbols) are the same as Figure 3b.

smaller than that (~–0.02 K/year) observed in the past seven years. After 2010 or so, a small bounce back in global temperature is expected to occur due to the small modulating effect arising from the 11 year cycles of cosmic rays interacting with CFCs leading to ozone depletion (Lu, 2010). However, a long-term trend of global cooling is expected for the coming five to seven decades.

5. **Concluding remarks**

In comparison with previous calculations on the greenhouse effect of CFCs, the present calculations give rise to a larger greenhouse effect. This is due to two factors: the former calculations significantly underestimated the amplification factor of water vapor feedbacks by using a much smaller β value of 0.15 (Ramanathan, 1975) and also overestimated the greenhouse effect of CO_2 by assuming a logarithmical increase in radiative forcing of CO_2 with increasing concentration (Ramanathan et al., 1985, 1998; IPCC, 2001, 2007). These should be revised with the present observations.

It should be noted that the application of the CO_2-palaeoclimate relation to the recent anthropogenic warming is questionable. Some studies reviewed in the IPCC Reports (2001, 2007) showed that CO_2 co-varied with Antarctic temperature over glacial-interglacial cycles, suggesting a close link between CO_2 variation and temperature. Ice core records, however,

indicate that the rise in atmospheric CO_2 is the effect rather than the cause of surface warming in palaeoclimate. For instance, a rapid rise by 5 °C in global average sea surface temperature occurred during transitions from the last Glacial Maximum to the onset of Holocene times; detailed ice core studies by Smith et al. (1999) found that the concentration of atmosphere CO_2 increased by about 80 ppm (from ~190 to 270 ppm). But the latter was due to the effect of the rise in global surface temperature on driving more CO_2 emission predominantly from the ocean (Smith et al., 1999). If one reversed the sequence and took the CO_2 increase as the cause of the 5 °C rise in global surface temperature, then it would be extremely difficult to understand why no global temperature increases were observed for the increases of atmospheric CO_2 from 285 to 308 ppm and 310 to 330 ppm in the decades from 1850 to 1930 and 1950 to 1975, respectively. In fact, high-resolution ice core records of temperature proxies and CO_2 during deglaciations generally show that Antarctic temperature started to rise *about one thousand years before* the rise of atmospheric CO_2, as well observed by Fischer et al. (1999), Veizer et al. (2000), Caillon et al. (2003) and Stott et al. (2007). And despite strongly decreasing temperatures, high CO_2 concentrations can be sustained *for thousands of years* during glaciations (Fischer et al., 1999). These facts indicate that atmospheric CO_2 was not the main cause of these climate transitions (Smith et al., 1999; Fischer et al., 1999; Veizer et al., 2000; Caillon et al., 2003; Stott et al., 2007).

Finally, accurate and reliable analysis of satellite datasets are often affected by the climate models that investigators use. This is to some extent caused by the complexity of the scientific issue, which might require the use of a certain climate model to guide the data analysis. On the other hand, researchers should also be aware of the fact that used climate models may be incorrect or incomplete. An open opinion about different models may be instrumental in revealing the truth. This study did not aim to make precise calculations of global temperature change with a sophisticated climate model including multiple parameters and factors. But it does show that the warming effect of CO_2 and other non-CFC gases had most likely saturated and CFCs and HCFCs could account for global warming observed in the late 20th century. A long-term global cooling starting around 2002 is expected to continue for next five to seven decades.

Acknowledgements

Global temperature data were from two sources, namely the UK Met Office Hadley Centre: the HadCRUT3 dataset, combined land-surface air temperature and sea-surface temperature anomalies (http://hadobs.metoffice.com/) and the US NOAA National Climatic Data Center (NCDC): the dataset of annual global (combined land and ocean temperature) anomalies (http://www.ncdc.noaa.gov/oa/climate/research/anomalies/index.html). CO_2 data from 1850 to 1958 were from the Law Dome DE08, DE08-2, and DSS ice core measurements (http://cdiac.ornl.gov/trends/co2/lawdome-data.html); for the years without recorded data, a linear extrapolation was used to obtain the CO_2 data between two closest recorded data points. CO_2 data after 1958 were from direct atmospheric measurements at Mauna Loa Observatory, Hawaii **(**http://www.esrl.noaa.gov/gmd/ccgg/trends/**).** Halocarbon concentrations were from the WMO Report (2007). This work is supported by the Canadian Institutes of Health Research (CIHR) and Natural Science and Engineering Research Council of Canada (NSERC).

References

Anderson, J. G., Dykema, J. A., Goody, R. M., Hua, H., Kirk-Davidoff, D. B. (2004). Absolute, spectrally-resolved, thermal radiance: a benchmark for climate monitoring from space. J. Quant. Spectrosc. & Radiat. Transfer, 85, 367-383.

Andrews, D. G. (2000). An Introduction to Atmospheric Physics. Cambridge University Press, Cambridge, UK.

Austin, J., Butchart, N., Shine, K. P. (1992). Possibility of an arctic ozone hole in a doubled-CO_2 climate. Nature, 360, 221-225.

Balling, R. C. (1992). The Heated Debate: greenhouse predictions versus climate reality. Pacific Research Institute for Public Policy.

Berk, A., Bernstein, L. S., Robertson, D. C. (1989). MODTRAN: A moderate resolution model for LOWTRAN 7, Air Force Geophysics Laboratory Technical Report GL-TR-89-0122, Hanscom, AFB, MA, pp.42.

Caillon, N., Severinghaus, J. P., Jouzel, J., Barnola, J.-M., Kang, J., Lipenkov, V. Y. (2003). Timing of Atmospheric CO2 and Antarctic Temperature Changes Across Termination III. Science, 299, 1728-1731.

Carslaw, K. S., Harrison, R. G., Kirkby, J. (2002). Cosmic rays, clouds, and climate, Science, 298, 1732-1737.

Clark, R. N. (1999) Chapter 1: Spectroscopy of Rocks and Minerals, and Principles of Spectroscopy. In: Rencz, A. N. (Eds.), Manual of Remote Sensing, Volume 3, Remote Sensing for the Earth Sciences, John Wiley and Sons, New York, pp.3-58.

Clerbaux, C., Hadji-Lazaro, J., Turquety, S., M´egie, G., Coheur P.-F. (2003). Trace gas measurements from infrared satellite for chemistry and climate applications. Atmos. Chem. Phys. Discuss., 3, 2027-2058.

Douglass, D. H., Pearson, B. D., Singer, S. F. (2004). Altitude dependence of atmospheric temperature trends: Climate models versus observation. Geophys. Res. Lett. 31, L13208.

Fischer, H., Wahlen, M., Smith, J., Mastroianni, D., Deck, B. (1999). Ice Core Records of Atmospheric CO2 Around the Last Three Glacial Terminations. Science, 283, 1712-1714.

Friis-Christensen, E., Lassen, K. (1991). Length of the Solar Cycle: An Indicator of Solar Activity Closely Associated with Climate. Science, 254, 698–700.

Goody, R., Anderson, J., North, G. (1998). Testing climate models: An approach. Bull. Am. Meteorol. Soc., 79, 2541-2549.

Griggs, J. A., Harries, J. E. (2007). Comparison of Spectrally Resolved Outgoing Longwave Radiation over the Tropical Pacific between 1970 and 2003 Using IRIS, IMG, and AIRS. J. Climate, 20, 3982-4001.

Hanel, R. A., Schlachman, B., Rogers, D., Vanous, D. (1971). The Nimbus 4 Michelson interferometer. Appl. Opt., 10**,** 1376-1382.

Harries, J. E., Brindley, H. E., Sagoo, P. J., Bantges, R. J. (2001). Increases in greenhouse forcing inferred from the outgoing longwave radiation spectra of the Earth in 1970 and 1997. Nature, 410, 355-357.

Idso, S. B. (1998). CO_2-induced global warming: a skeptic's view of potential climate change. Clim. Res., 10, 69-82.

IPCC (2001). *Third Assessment Report: Climate Change (TAR).*

IPCC (2007). *Fourth Assessment Report: Climate Change (AR4).*

Kidder, S. Q., Vonder Haar, T. H. (1995). Satellite Meteorology: An Introduction. Academic Press, San Diego, US.

Kobayashi, H., Shimota, A., Kondo, K., Okumura, E., Kameda, Y., Shimoda, H., Ogawa, T. (1999). Development and evaluation of the interferometric monitor for greenhouse gases: a high-throughput Fourier-transform infrared radiometer for nadir Earth observation. Appl. Opt., 38, 6801-6807.

Lindzen, R. S. (1997). Can increasing carbon dioxide cause climate change? Proc. Natl. Acad. Sci. USA, 94, 8335-8342.

Lu, Q.-B., (2009). Correlation between Cosmic Rays and Ozone Depletion. Phys. Rev. Lett., 102, 118501(1-4).

Lu, Q.-B. (2010). Cosmic-Ray-Driven Electron-Induced Reactions of Halogenated Molecules Adsorbed on Ice Surfaces: Implications for Atmospheric Ozone Depletion and Global Climate Change. Phys. Rep., 487, 141-167.

Overduin, J. M. (2003). Eyesight and the solar Wien peak. Am. J. Phys., 71, 216-219.

Ramanathan, V. (1975). Greenhouse Effect Due to Chlorofluorocarbons: Climatic Implications. Science, 190, 50-52.

Ramanathan, V., Cicerone, R. J., Singh, H. B., Kiehl, J. T. (1985). Trace Gas Trends and Their Potential Role in Climate Change. J. Geophys. Res., 90, 5547-5566.

Ramanathan, V. (1998). Trace Gas Greenhouse Effect and Global Warming, Underlying Principles and Outstanding Issues. *Ambio*, 27, 187-197.

Ratkowski, A. J., Anderson, G. P., Chetwynd, J. H., Nadile, R. M., Devir, A. D., Conley, T. D. (1998). Paper presented at the RTO SET Symposium on "E-O Propagation, Signature and System Performance Under Adverse Meteorological Conditions Considering Out-of-Area Operations" (Italian Air Force Academy, Naples, Italy) and published in RTO MP-I.

Shindell, D. T., Rind, D., Lonergan, P. (1998). Increased polar stratospheric ozone losses and delayed eventual recovery owing to increasing greenhouse-gas concentrations. Nature**,** 392, 589-593.

Schneider, C. W., Kucerovsky, Z., Brannen, E. (1989). Carbon dioxide absorption of He-Ne laser radiation at 4.2 μm: characteristics of self and nitrogen broadened cases. Appl. Opt., 28, 959-966.

Smith, H. J., Fischer, H., Wahlen, M., Mastroianni, D., Deck, B. (1999). Dual modes of the carbon cycle since the Last Glacial Maximum. Nature**,** 400, 248-250.

Soffer, B. H., Lynch, D. K. (1999). Some paradoxes, errors, and resolutions concerning the spectral optimization of human vision. Am. J. Phys., 67**,** 946-953.

Soon, W., Baliunas, S., Idso, S. B., Kondratyev, K. Y., Posmentier, E. S. (2001). Modeling climatic effects of anthropogenic carbon dioxide emissions: unknowns and uncertainties. Clim. Res., 18, 259-275.

Stott, L., Timmermann, A., Thunell, R. (2007). Southern Hemisphere and Deep-Sea Warming Led Deglacial Atmospheric CO_2 Rise and Tropical Warming. Science, 318, 435-438.

Svensmark, H., Friis-Christensen, E. (1997). Variation of cosmic ray flux and global cloud coverage - A missing link in solar-climate relationships. J. Atmos. Sol.-Terr. Phys., 59, 1225-1232.

Veizer, J., Godderis, Y., Francois, L. M. (2000). Evidence for decoupling of atmospheric CO_2 and global climate during the Phanerozoiceon. Nature, 408, 698-701.

Wang, J. X., Anderson G. P., Revercomb H. E., Knuteson R. O. (1996). Validation of FASCOD3 and MODTRAN3: Comparison of model calculations with ground-based and airborne interferometer observations under clear-sky conditions. Appl. Opt., 35**,** 6028-6040.

Wang, W.-C. and Molnar G. (1985). A Model Study of the Greenhouse Effects Due to Increasing Atmospheric CH_4, N_2O, CF_2Cl_2, and $CFCl_3$. J. Geophys. Res., 90, 12971-12980.

World Meteorological Organization (WMO) (1999). Scientific Assessment of Ozone Depletion: 1998 (Global Ozone Research and Monitoring Project-Report No. 44, Geneva) Chap 12.

World Meteorological Organization (WMO) (2007). Scientific Assessment of Ozone Depletion: 2006 (Global Ozone Research and Monitoring Project-Report No. 50, Geneva) Chap 8.